Chapter 5

Model Neurons I: Neuroelectronics

5.1 Introduction

A great deal is known about the biophysical mechanisms responsible for generating neuronal activity, and these provide a basis for constructing neuron models. Such models range from highly detailed descriptions involving thousands of coupled differential equations to greatly simplified caricatures useful for studying large interconnected networks. In this chapter, we discuss the basic electrical properties of neurons and the mathematical models by which they are described. We present a simple but nevertheless useful model neuron, the integrate-and-fire model, in a basic version and with added membrane and synaptic conductances. We also discuss the Hodgkin-Huxley model, which describes the conductances responsible for generating action potentials. In chapter 6, we continue by presenting more complex models, both in terms of their conductances and their morphology. Circuits and networks of model neurons are discussed in chapter 7. This chapter makes use of basic concepts of electrical circuit theory, which are reviewed in the Mathematical Appendix.

5.2 Electrical Properties of Neurons

Like other cells, neurons are packed with a huge number and variety of ions and molecules. A cubic micron of cytoplasm might contain, for example, 10^{10} water molecules, 10^8 ions, 10^7 small molecules such as amino acids and nucleotides, and 10^5 proteins. Many of these molecules carry charges, either positive or negative. Most of the time, there is an excess concentration of negative charge inside a neuron. Excess charges that are

mobile, like ions, repel each other and build up on the inside surface of the cell membrane. Electrostatic forces attract an equal density of positive ions from the extracellular medium to the outside surface of the membrane.

cell membrane

The cell membrane is a lipid bilayer 3 to 4 nm thick that is essentially impermeable to most charged molecules. This insulating feature causes the cell membrane to act as a capacitor by separating the charges lying along its interior and exterior surfaces. Numerous ion-conducting channels embedded in the cell membrane (figure 5.1) lower the effective membrane resistance for ion flow to a value about 10,000 times smaller than that of a pure lipid bilayer. The resulting membrane conductance depends on the density and types of ion channels. A typical neuron may have a dozen or more different types of channels, anywhere from a few to hundreds of channels in a square micron of membrane, and hundreds of thousands to millions of channels in all. Many, but not all, channels are highly selective, allowing only a single type of ion to pass through them (to an accuracy of about 1 ion in 10^4). The capacity of channels for conducting ions across the cell membrane can be modified by many factors including the membrane potential (voltage-dependent channels), the internal concentration of various intracellular messengers (Ca^{2+}-dependent channels, for example), and the extracellular concentration of neurotransmitters or neuromodulators (synaptic receptor channels, for example). The membrane also contains selective pumps that expend energy to maintain differences in the concentrations of ions inside and outside the cell.

ion channels

channel selectivity

ion pumps

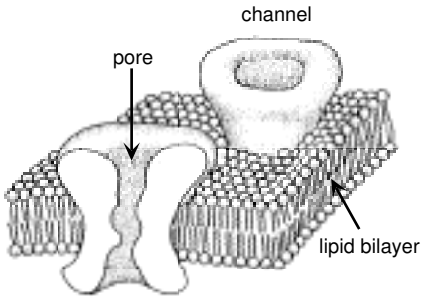

Figure 5.1: A schematic diagram of a section of the lipid bilayer that forms the cell membrane with two ion channels embedded in it. The membrane is 3 to 4 nm thick and the ion channels are about 10 nm long. (Adapted from Hille, 1992.)

membrane potential

By convention, the potential of the extracellular fluid outside a neuron is defined to be zero. When a neuron is inactive, the excess internal negative charge causes the potential inside the cell membrane to be negative. This potential is an equilibrium point at which the flow of ions into the cell matches that out of the cell. The potential can change if the balance of ion flow is modified by the opening or closing of ion channels. Under normal conditions, neuronal membrane potentials vary over a range from about -90 to +50 mV. The order of magnitude of these potentials can be estimated from basic physical principles.

Membrane potentials are small enough to allow neurons to take advantage of thermal energy to help transport ions across the membrane, but are large enough so that thermal fluctuations do not swamp the signaling capabilities of the neuron. These conditions imply that potential differences across the cell membrane must lie in a range so that the energy gained or lost by an ion traversing the membrane is the same order of magnitude as its thermal energy. The thermal energy of an ion is about $k_B T$ where k_B is the Boltzmann constant and T is the temperature on an absolute Kelvin scale. For chemists and biologists (though not for physicists), it is more customary to discuss moles of ions rather than single ions. A mole of ions has Avagadro's number times as much thermal energy as a single ion, or RT, where R is the universal gas constant, equal to 8.31 joules/mol K° = 1.99 cal/mol K°. RT is about 2500 joules/mol or 0.6 kCal/mol at normal temperatures. To estimate the size of typical membrane potentials, we equate this to the energy gained or lost when a mole of ions crosses a membrane with a potential difference V_T across it. This energy is FV_T where F is the Faraday constant, F = 96,480 Coulombs/mol, equal to Avagadro's number times the charge of a single proton, q. Setting $FV_T = RT$ gives

V_T

$$V_T = \frac{RT}{F} = \frac{k_B T}{q}. \tag{5.1}$$

This is an important parameter that enters into a number of calculations. V_T is between 24 and 27 mV for the typical temperatures of cold and warm-blooded animals. This sets the overall scale for membrane potentials across neuronal membranes, which range from about -3 to +2 times V_T.

Intracellular Resistance

Membrane potentials measured at different places within a neuron can take different values. For example, the potentials in the soma, dendrite, and axon can all be different. Potential differences between different parts of a neuron cause ions to flow within the cell, which tends to equalize these differences. The intracellular medium provides a resistance to such flow. This resistance is highest for long and narrow stretches of dendritic or axonal cable, such as the segment shown in figure 5.2. The longitudinal current I_L flowing along such a cable segment can be computed from Ohm's law. For the cylindrical segment of dendrite shown in figure 5.2, the longitudinal current flowing from right to left satisfies $V_2 - V_1 = I_L R_L$. Here, R_L is the longitudinal resistance, which grows in proportion to the length of the segment (long segments have higher resistances than short ones) and is inversely proportional to the cross-sectional area of the segment (thin segments have higher resistances than fat ones). The constant of proportionality is called the intracellular resistivity, r_L, and it typically falls in a range from 1 to 3 kΩ·mm. The longitudinal resistance of the segment in figure 5.2 is r_L times the length L divided by the cross-sectional

longitudinal current I_L

longitudinal resistance R_L

intracellular resistivity r_L

area πa^2, $R_L = r_L L/\pi a^2$. A segment 100 μm long with a radius of 2 μm has a longitudinal resistance of about 8 MΩ. A voltage difference of 8 mV would be required to force 1 nA of current down such a segment.

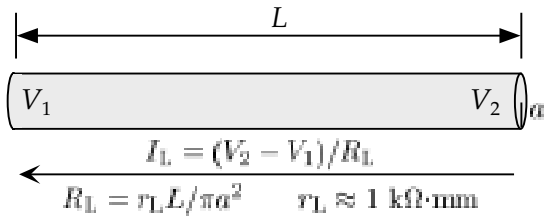

Figure 5.2: The longitudinal resistance of a cylindrical segment of neuronal cable with length L and radius a. The difference between the membrane potentials at either end of this segment is related to the longitudinal current within the segment by Ohm's law, with R_L the longitudinal resistance of the segment. The arrow indicates the direction of positive current flow. The constant r_L is the intracellular resistivity, and a typical value is given.

single-channel conductance

We can also use the intracellular resistivity to estimate crudely the conductance of a single channel. The conductance, being the inverse of a resistance, is equal to the cross-sectional area of the channel pore divided by its length and by r_L We approximate the channel pore as a tube of length 6 nm and opening area 0.15 nm^2. This gives an estimate of 0.15 nm ^{2}/(1 kΩ mm $\times$ 6 nm) $\approx$ 25 pS, which is the right order of magnitude for a channel conductance.

Membrane Capacitance and Resistance

electrotonic compactness

The intracellular resistance to current flow can cause substantial differences in the membrane potential measured in different parts of a neuron, especially during rapid transient excursions of the membrane potential from its resting value, such as action potentials. Neurons that have few of the long and narrow cable segments that produce high longitudinal resistance may have relatively uniform membrane potentials across their surfaces. Such neurons are termed electrotonically compact. For electrotonically compact neurons, or for less compact neurons in situations where spatial variations in the membrane potential are not thought to play an important functional role, the entire neuron may be adequately described by a single membrane potential. Here, we discuss the membrane capacitance and resistance using such a description. An analysis for the case of spatially varying membrane potentials is presented in chapter 6.

membrane capacitance C_m

We have mentioned that there is typically an excess negative charge on the inside surface of the cell membrane of a neuron, and a balancing positive charge on its outside surface (figure 5.3). In this arrangement, the cell membrane creates a capacitance C_m, and the voltage across the mem-

brane V and the amount of this excess charge Q are related by the standard equation for a capacitor, $Q = C_{\rm m}V$. The membrane capacitance is proportional to the total amount of membrane or, equivalently, to the surface area of the cell. The constant of proportionality, called the specific membrane capacitance, is the capacitance per unit area of membrane, and is approximately the same for all neurons, $c_{\rm m} \approx 10$ nF/mm^2. The total capacitance $C_{\rm m}$ is the membrane surface area A times the specific capacitance, $C_{\rm m} = c_{\rm m}A$. Neuronal surface areas tend to be in the range 0.01 to 0.1 mm^2, so the membrane capacitance for a whole neuron is typically 0.1 to 1 nF. For a neuron with a total membrane capacitance of 1 nF, 7×10^{-11} C or about 10^9 singly charged ions are required to produce a resting potential of -70 mV. This is about a hundred-thousandth of the total number of ions in a neuron and is the amount of charge delivered by a 0.7 nA current in 100 ms.

specific membrance capacitance c_m

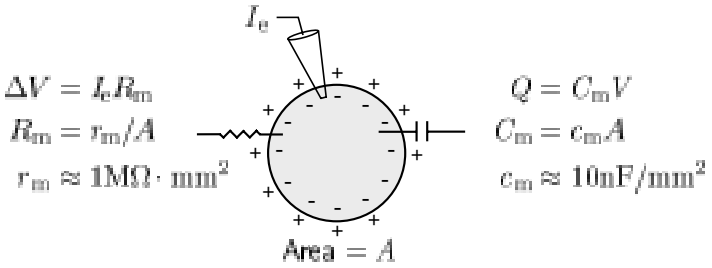

Figure 5.3: The capacitance and membrane resistance of a neuron considered as a single compartment. The membrane capacitance determines how the membrane potential V and excess internal charge Q are related. The membrane resistance $R_{\rm m}$ determines the size of the membrane potential deviation ΔV caused by a small current $I_{\rm e}$ entering through an electrode, for example. Equations relating the total membrane capacitance and resistance, $C_{\rm m}$ and $R_{\rm m}$, to the specific membrane capacitance and resistance, $c_{\rm m}$ and $r_{\rm m}$, are given along with typical values of $c_{\rm m}$ and $r_{\rm m}$. The value of $r_{\rm m}$ may vary considerably under different conditions and for different neurons.

We can use the membrane capacitance to determine how much current is required to change the membrane potential at a given rate. The time derivative of the basic equation relating the membrane potential and charge,

$$C_{\rm m}\frac{dV}{dt} = \frac{dQ}{dt}\,, \tag{5.2}$$

plays an important role in the mathematical modeling of neurons. The time derivative of the charge dQ/dt is equal to the current passing into the cell, so the amount of current needed to change the membrane potential of a neuron with a total capacitance $C_{\rm m}$ at a rate dV/dt is $C_{\rm m}dV/dt$. For example, 1 nA will change the membrane potential of a neuron with a capacitance of 1 nF at a rate of 1 mV/ms.

The capacitance of a neuron determines how much current is required to make the membrane potential change at a given rate. Holding the membrane potential steady at a level different from its resting value also requires current, but this current is determined by the membrane resistance rather than by the capacitance of the cell. For example, if a small constant current I_e is injected into a neuron through an electrode, as in figure 5.3, the membrane potential will shift away from its resting value by an amount ΔV given by Ohm's law, $\Delta V = I_e R_m$. R_m is known as the membrane or input resistance. The restriction to small currents and small ΔV is required because membrane resistances can vary as a function of voltage, whereas Ohm's law assumes R_m is constant over the range ΔV.

membrane resistance R_m

membrane conductance

specific membrane resistance r_m

The membrane resistance is the inverse of the membrane conductance, and, like the capacitance, the conductance of a piece of cell membrane is proportional to its surface area. The constant of proportionality is the membrane conductance per unit area, but we write it as $1/r_m$, where r_m is called the specific membrane resistance. Conversely, the membrane resistance R_m is equal to r_m divided by the surface area. When a neuron is in a resting state, the specific membrane resistance is around 1 M$\Omega\cdot$mm^2. This number is much more variable than the specific membrane capacitance. Membrane resistances vary considerably among cells and under different conditions and at different times for a given neuron, depending on the number, type, and state of its ion channels. For total surface areas between 0.01 and 0.1 mm, the membrane resistance is typically in the range 10 to 100 MΩ. With a 100 MΩ membrane resistance, a constant current of 0.1 nA is required to hold the membrane potential 10 mV away from its resting value.

membrane time constant τ_m

The product of the membrane capacitance and the membrane resistance is a quantity with the units of time called the membrane time constant, $\tau_m = R_m C_m$. Because C_m and R_m have inverse dependences on the membrane surface area, the membrane time constant is independent of area and equal to the product of the specific membrane capacitance and resistance, $\tau_m = r_m c_m$. The membrane time constant sets the basic time scale for changes in the membrane potential and typically falls in the range between 10 and 100 ms.

Equilibrium and Reversal Potentials

Electric forces and diffusion are responsible for driving ions through channel pores. Voltage differences between the exterior and interior of the cell produce forces on ions. Negative membrane potentials attract positive ions into the neuron and repel negative ions. In addition, ions diffuse through channels because the ion concentrations differ inside and outside the neuron. These differences are maintained by the ion pumps within the cell membrane. The concentrations of Na^+ and Ca^{2+} are higher outside the cell than inside, so these ions are driven into the neuron by diffusion. K^+

is more concentrated inside the neuron than outside, so it tends to diffuse out of the cell.

It is convenient to characterize the current flow due to diffusion in terms of an equilibrium potential. This is defined as the membrane potential at which current flow due to electric forces cancels the diffusive flow. For channels that conduct a single type of ion, the equilibrium potential can be computed easily. The potential difference across the cell membrane biases the flow of ions into or out of a neuron. Consider, for example, a positively charged ion and a negative membrane potential. In this case, the membrane potential opposes the flow of ions out of the the cell. Ions can only cross the membrane and leave the interior of the cell if they have sufficient thermal energy to overcome the energy barrier produced by the membrane potential. If the ion has an electric charge zq where q is the charge of one proton, it must have a thermal energy of at least $-zqV$ to cross the membrane (this is a positive energy for $z > 0$ and $V < 0$). The probability that an ion has a thermal energy greater than or equal to $-zqV$, when the temperature (on an absolute scale) is T, is $\exp(zqV/k_{\rm B}T)$. This is determined by integrating the Boltzmann distribution for energies greater than or equal to $-zqV$. In molar units, this result can be written as $\exp(zFV/RT)$, which is equal to $\exp(zV/V_T)$ by equation 5.1.

equilibrium potential

The biasing effect of the electrical potential can be overcome by an opposing concentration gradient. A concentration of ions inside the cell, [inside], that is sufficiently greater than the concentration outside the cell, [outside], can compensate for the Boltzmann probability factor. The rate at which ions flow into the cell is proportional to [outside]. The flow of ions out of the cell is proportional to [inside] times the Boltzmann factor, because in this direction only those ions that have sufficient thermal energy can leave the cell. The net flow of ions will be zero when the inward and outward flows are equal. We use the letter E to denote the particular potential that satisfies this balancing condition, which is then

$$[\text{outside}] = [\text{inside}] \exp(zE/V_T) \,. \tag{5.3}$$

Solving this equation for E, we find

Nernst equation

$$E = \frac{V_T}{z} \ln\left(\frac{[\text{outside}]}{[\text{inside}]}\right) . \tag{5.4}$$

Equation 5.4 is the Nernst equation. The reader can check that, if the result is derived for either sign of ionic charge or membrane potential, the result is identical to 5.4, which thus applies in all cases. Equilibrium potentials for K^+ channels, labeled $E_{\rm K}$, typically fall in the range between -70 and -90 mV. Na^+ equilibrium potentials, $E_{\rm Na}$, are 50 mV or higher, and $E_{\rm Ca}$ for Ca^{2+} channels is higher still, around 150 mV. Finally, Cl^- equilibrium potentials are typically around -60 to -65 mV, near the resting potential of many neurons.

The Nernst equation (5.4) applies when the channels that generate a particular conductance allow only one type of ion to pass through them. Some

channels are not so selective, and in this case the potential E is not determined by equation 5.4, but rather takes a value intermediate between the equilibrium potentials of the individual ion types that it conducts. An approximate formula known as the Goldman equation (see Tuckwell, 1988; or Johnston and Wu, 1995) can be used to estimate E for such conductances. In this case, E is often called a reversal potential, rather than an equilibrium potential, because the direction of current flow through the channel switches as the membrane potential passes through E.

Goldman equation

reversal potential

A conductance with an equilibrium or reversal potential E tends to move the membrane potential of the neuron toward the value E. When $V > E$ this means that positive current will flow outward, and when $V < E$ positive current will flow inward. Because Na^+ and Ca^{2+} conductances have positive reversal potentials, they tend to depolarize a neuron (make its membrane potential less negative). K^+ conductances, with their negative E values, normally hyperpolarize a neuron (make its membrane potential more negative). Cl^- conductances with reversal potentials near the resting potential, may pass little net current. Instead, their primary impact is to change the membrane resistance of the cell. Such conductances are sometimes called shunting, although all conductances 'shunt', that is, increase the total conductance of a neuron. Synaptic conductances are also characterized by reversal potentials and are termed excitatory or inhibitory on this basis. Synapses with reversal potentials less than the threshold for action potential generation are typically called inhibitory, while those with more depolarizing reversal potentials are called excitatory.

depolarization

hyperpolarization

shunting conductances

inhibitory and excitatory synapses

The Membrane Current

The total current flowing across the membrane through all of its ion channels is called the membrane current of the neuron. By convention, the membrane current is defined as positive when positive ions leave the neuron and negative when positive ions enter the neuron. The total membrane current is determined by summing currents due to all of the different types of channels within the cell membrane, including voltage-dependent and synaptic channels. To facilitate comparisons between neurons of different sizes, it is convenient to use the membrane current per unit area of cell membrane, which we call $i_{\rm m}$. The total membrane current is obtained from $i_{\rm m}$ by multipling it by A the total surface area of the cell.

membrane current per unit area i_m

We label the different types of channels in a cell membrane with an index i. As discussed in the last section, the current carried by a set of channels of type i with reversal potential E_i, vanishes when the membrane potential satisfies $V = E_i$. For many types of channels, the current increases or decreases approximately linearly when the membrane potential deviates from this value. The difference $V - E_i$ is called the driving force, and the membrane current per unit area due to the type i channels is written as $g_i(V - E_i)$. The factor g_i is the conductance per unit area due to these

driving force

conductance per unit area g_i

channels. Summing over the different types of channels, we obtain the total membrane current

membrane current

$$i_{\rm m} = \sum_i g_i(V - E_i)\,. \tag{5.5}$$

Sometimes a more complicated expression called the Goldman-Hodgkin-Katz formula is used to relate the membrane current to g_i and membrane potential (see Tuckwell, 1988; or Johnston and Wu, 1995), but we will restrict our discussion to the simpler relationship used in equation 5.5.

Much of the complexity and richness of neuronal dynamics arises because membrane conductances change over time. However, some of the factors that contribute to the total membrane current can be treated as relatively constant, and these are typically grouped together into a single term called the leakage current. The currents carried by ion pumps that maintain the concentration gradients that make equilibrium potentials nonzero typically fall into this category. For example, one type of pump uses the energy of ATP hydrolysis to move three Na^+ ions out of the cell for every two K^+ ions it moves in. It is normally assumed that these pumps work at relatively steady rates so that the currents they generate can be included in a time-independent leakage conductance. Sometimes, this assumption is dropped and explicit pump currents are modeled. In either case, all of the time-independent contributions to the membrane current can be lumped together into a single leakage term $\overline{g}_{\rm L}(V - E_{\rm L})$. Because this term hides many sins, its reversal potential $E_{\rm L}$ is not usually equal to the equilibrium potential of any specific ion. Instead it is often kept as a free parameter and adjusted to make the resting potential of the model neuron match that of the cell being modeled. Similarly, $\overline{g}_{\rm L}$ is adjusted to match the membrane conductance at rest. The line over the parameter $\overline{g}_{\rm L}$ is used to indicate that it has constant value. A similar notation is used later in this chapter to distinguish variable conductances from the fixed parameters that describe them. The leakage conductance is called a passive conductance to distinguish it from variable conductances that are termed active.

leakage current

resting potential

5.3 Single-Compartment Models

Models that describe the membrane potential of a neuron by a single variable V are called single-compartment models. This chapter deals exclusively with such models. Multi-compartment models, which can describe spatial variations in the membrane potential, are considered in chapter 6. The equations for single-compartment models, like those of all neuron models, describe how charges flow into and out of a neuron and affect its membrane potential.

Equation 5.2 provides the basic relationship that determines the membrane potential for a single-compartment model. This equation states that the rate of change of the membrane potential is proportional to the rate

at which charge builds up inside the cell. The rate of charge buildup is, in turn, equal to the total amount of current entering the neuron. The relevant currents are those arising from all the membrane and synaptic conductances plus, in an experimental setting, any current injected into the cell through an electrode. From equation 5.2, the sum of these currents is equal to $C_m dV/dt$, the total capacitance of the neuron times the rate of change of the membrane potential. Because the membrane current is usually characterized as a current per unit area, i_m, it is more convenient to divide this relationship by the surface area of the neuron. Then, the total current per unit area is equal to $c_m dV/dt$, where $c_m = C_m/A$ is the specific membrane capacitance. One complication in this procedure is that the electrode current, I_e is not typically expressed as a current per unit area, so we must divide it by the total surface area of the neuron, A. Putting all this together, the basic equation for all single-compartment models is

single-compartment model

$$c_m \frac{dV}{dt} = -i_m + \frac{I_e}{A}\,. \tag{5.6}$$

By convention, current that enters the neuron through an electrode is defined as positive-inward, whereas membrane current is defined as positive-outward. This explains the different signs for the currents in equation 5.6. The membrane current in equation 5.6 is determined by

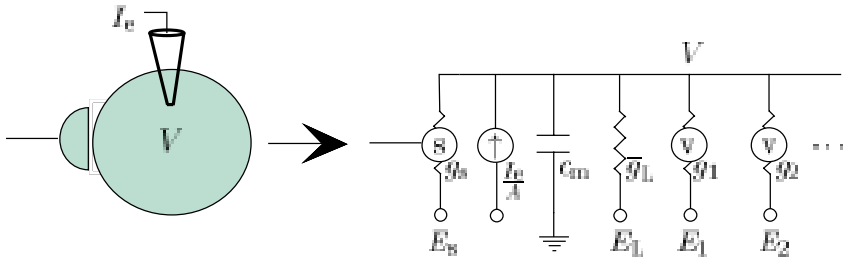

Figure 5.4: The equivalent circuit for a one-compartment neuron model. The neuron is represented, at the left, by a single compartment of surface area A with a synapse and a current injecting electrode. At right is the equivalent circuit. The circled (S) indicates a synaptic conductance that depends on the activity of a presynaptic neuron. A single synaptic conductance g_s is indicated, but, in general, there may be several different types. The circled (V) indicates a voltage-dependent conductance, and I_e is the current passing through the electrode, The dots stand for possible additional membrane conductances.

equation 5.5 and additional equations that specify the conductance variables g_i. The structure of such a model is the same as that of an electrical circuit, called the equivalent circuit, consisting of a capacitor and a set of variable and non-variable resistors corresponding to the different membrane conductances. Figure 5.4 shows the equivalent circuit for a generic one-compartment model.

equivalent circuit

5.4 Integrate-and-Fire Models

A neuron will typically fire an action potential when its membrane potential reaches a threshold value of about -55 to -50 mV. During the action potential, the membrane potential follows a rapid stereotyped trajectory and then returns to a value that is hyperpolarized relative to the threshold potential. As we will see, the mechanisms by which voltage-dependent K^+ and Na^+ conductances produce action potentials are well-understood and can be modeled quite accurately. On the other hand, neuron models can be simplified and simulations can be accelerated dramatically if the biophysical mechanisms responsible for action potentials are not explicitly included in the model. Integrate-and-fire models do this by stipulating that an action potential occurs whenever the membrane potential of the model neuron reaches a threshold value $V_{\rm th}$. After the action potential, the potential is reset to a value $V_{\rm reset}$ below the threshold potential, $V_{\rm reset} < V_{\rm th}$.

integrate and fire model

The basic integrate-and-fire model was proposed by Lapicque in 1907, long before the mechanisms that generate action potentials were understood. Despite its age and simplicity, the integrate-and-fire model is still an extremely useful description of neuronal activity. By avoiding a biophysical description of the action potential, integrate-and-fire models are left with the simpler task of modeling only subthreshold membrane potential dynamics. This can be done with various levels of rigor. In the simplest version of these models, all active membrane conductances are ignored, including, for the moment, synaptic inputs, and the entire membrane conductance is modeled as a single passive leakage term, $i_{\rm m} = \overline{g}_{\rm L}(V - E_{\rm L})$. This version is called the passive or leaky integrate-and-fire model. For small fluctuations about the resting membrane potential, neuronal conductances are approximately constant, and the passive integrate-and-fire model assumes that this constancy holds over the entire subthreshold range. For some neurons this is a reasonable approximation, and for others it is not. With these approximations, the model neuron behaves like an electric circuit consisting of a resistor and a capacitor in parallel (figure 5.4), and the membrane potential is determined by equation 5.6 with $i_{\rm m} = \overline{g}_{\rm L}(V - E_{\rm L})$,

$$c_{\rm m}\frac{dV}{dt} = -\overline{g}_{\rm L}(V - E_{\rm L}) + \frac{I_{\rm e}}{A}\,. \tag{5.7}$$

It is convenient to multiply equation 5.7 by the specific membrane resistance $r_{\rm m}$, which in this case is given by $r_{\rm m} = 1/\overline{g}_{\rm L}$. This cancels the factor of $\overline{g}_{\rm L}$ on the right side of the equation and leaves a factor $c_{\rm m}r_{\rm m} = \tau_{\rm m}$ on the left side, where $\tau_{\rm m}$ is the membrane time constant of the neuron. The electrode current ends up being multiplied by $r_{\rm m}/A$ which is the total membrane resistance $R_{\rm m}$. Thus, the basic equation of the passive integrate-and-fire models is

passive integrate-and-fire model

$$\tau_{\rm m}\frac{dV}{dt} = E_{\rm L} - V + R_{\rm m}I_{\rm e}\,. \tag{5.8}$$

To generate action potentials in the model, equation 5.8 is augmented by the rule that whenever V reaches the threshold value $V_{\rm th}$, an action potential is fired and the potential is reset to $V_{\rm reset}$. Equation 5.8 indicates that when $I_{\rm e} = 0$, the membrane potential relaxes exponentially with time constant $\tau_{\rm m}$ to $V = E_{\rm L}$. Thus, $E_{\rm L}$ is the resting potential of the model cell.

The membrane potential for the passive integrate-and-fire model is determined by integrating equation 5.8 (a numerical method for doing this is described in appendix A) and applying the threshold and reset rule for action potential generation. The response of a passive integrate-and-fire model neuron to a time-varying electrode current is shown in figure 5.5.

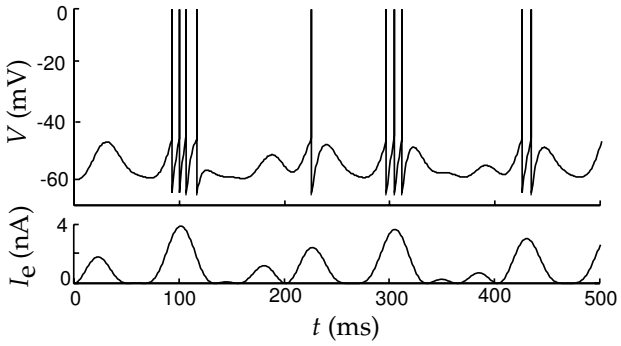

Figure 5.5: A passive integrate-and-fire model driven by a time-varying electrode current. The upper trace is the membrane potential and the bottom trace the driving current. The action potentials in this figure are simply pasted onto the membrane potential trajectory whenever it reaches the threshold value. The parameters of the model are $E_{\rm L} = V_{\rm reset} = -65$ mV, $V_{\rm th} = -50$ mV, $\tau_{\rm m} = 10$ ms, and $R_{\rm m} = 10$ MΩ.

The firing rate of an integrate-and-fire model in response to a constant injected current can be computed analytically. When $I_{\rm e}$ is independent of time, the subthreshold potential $V(t)$ can easily be computed by solving equation 5.8 and is

$$V(t) = E_{\rm L} + R_{\rm m} I_{\rm e} + (V(0) - E_{\rm L} - R_{\rm m} I_{\rm e}) \exp(-t/\tau_{\rm m}) \qquad (5.9)$$

where $V(0)$ is the value of V at time $t = 0$. This solution can be checked simply by substituting it into equation 5.8. It is valid for the integrate-and-fire model only as long as V stays below the threshold. Suppose that at $t = 0$, the neuron has just fired an action potential and is thus at the reset potential, so that $V(0) = V_{\rm reset}$. The next action potential will occur when the membrane potential reaches the threshold, that is, at a time $t = t_{\rm isi}$ when

$$V(t_{\rm isi}) = V_{\rm th} = E_{\rm L} + R_{\rm m} I_{\rm e} + (V_{\rm reset} - E_{\rm L} - R_{\rm m} I_{\rm e}) \exp(-t_{\rm isi}/\tau_{\rm m}) \,. \qquad (5.10)$$

By solving this for $t_{\rm isi}$, the time of the next action potential, we can determine the interspike interval for constant $I_{\rm e}$, or equivalently its inverse,

which we call the interspike-interval firing rate of the neuron,

$$r_{\rm isi} = \frac{1}{t_{\rm isi}} = \left[\tau_{\rm m} \ln\left(\frac{R_{\rm m} I_{\rm e} + E_{\rm L} - V_{\rm reset}}{R_{\rm m} I_{\rm e} + E_{\rm L} - V_{\rm th}}\right)\right]^{-1} . \tag{5.11}$$

This expression is valid if $R_{\rm m} I_{\rm e} > V_{\rm th} - E_{\rm L}$, otherwise $r_{\rm isi} = 0$. For sufficiently large values of $I_{\rm e}$, we can use the linear approximation of the logarithm ($\ln(1+z) \approx z$ for small z) to show that

$$r_{\rm isi} \approx \left[\frac{E_{\rm L} - V_{\rm th} + R_{\rm m} I_{\rm e}}{\tau_{\rm m}(V_{\rm th} - V_{\rm reset})}\right]_+ , \tag{5.12}$$

which shows that the firing rate grows linearly with $I_{\rm e}$ for large $I_{\rm e}$.

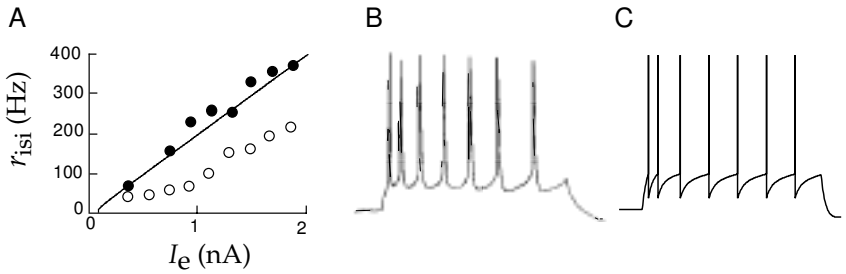

Figure 5.6: A) Comparison of interspike-interval firing rates as a function of injected current for an integrate-and-fire model and a cortical neuron measure *in vivo*. The line gives $r_{\rm isi}$ for a model neuron with $\tau_{\rm m} = 30$ ms, $E_{\rm L} = V_{\rm reset} = -65$ mV, $V_{\rm th} = -50$ mV and $R_{\rm m} = 90$ MΩ. The data points are from a pyramidal cell in the primary visual cortex of a cat. The filled circles show the inverse of the interspike interval for the first two spikes fired, while the open circles show the steady-state interspike-interval firing rate after spike-rate adaptation. B) A recording of the firing of a cortical neuron under constant current injection showing spike-rate adaptation. C) Membrane voltage trajectory and spikes for an integrate-and-fire model with an added current with $r_{\rm m}\Delta g_{\rm sra}$ = 0.06, $\tau_{\rm sra}$ = 100 ms, and $E_{\rm K}$ = -70 mV (see equations 5.13 and 5.14). (Data in A from Ahmed et al., 1998, B from McCormick, 1990.)

Figure 5.6A compares $r_{\rm isi}$ as a function of $I_{\rm e}$, using appropriate parameter values, with data from current injection into a cortical neuron *in vivo*. The firing rate of the cortical neuron in figure 5.6A has been defined as the inverse of the interval between pairs of spikes. The rates determined in this way using the first two spikes fired by the neuron in response to the injected current (filled circles in figure 5.6A) agree fairly well with the results of the integrate-and-fire model with the parameters given in the figure caption. However, the real neuron exhibits spike-rate adaptation, in that the interspike intervals lengthen over time when a constant current is injected into the cell (figure 5.6B) before settling to a steady-state value. The steady-state firing rate in figure 5.6A (open circles) could also be fit by an integrate-and-fire model, but not using the same parameters as were used to fit the initial spikes. Spike-rate adaptation is a common feature of

spike-rate adaptation

cortical pyramidal cells, and consideration of this phenomenon allows us to show how an integrate-and-fire model can be modified to incorporate more complex dynamics.

Spike-Rate Adaptation and Refractoriness

The passive integrate-and-fire model that we have described thus far is based on two separate approximations, a highly simplified description of the action potential and a linear approximation for the total membrane current. If details of the action potential generation process are not important for a particular modeling goal, the first approximation can be retained while the membrane current is modeled in as much detail as is necessary. We will illustrate this process by developing a heuristic description of spike-rate adaptation using a model conductance that has characteristics similar to measured neuronal conductances known to play important roles in producing this effect.

We model spike-rate adaptation by including an additional current in the model,

$$\tau_{\rm m}\frac{dV}{dt} = E_{\rm L} - V - r_{\rm m}g_{\rm sra}(V - E_K) + R_{\rm m}I_{\rm e}\,. \tag{5.13}$$

The spike-rate adaptation conductance $g_{\rm sra}$ has been modeled as a K^+ conductance so, when activated, it will hyperpolarize the neuron, slowing any spiking that may be occurring. We assume that this conductance relaxes to zero exponentially with time constant $\tau_{\rm sra}$ through the equation

$$\tau_{\rm sra}\frac{dg_{\rm sra}}{dt} = -g_{\rm sra}\,. \tag{5.14}$$

Whenever the neuron fires a spike, $g_{\rm sra}$ is increased by an amount $\Delta g_{\rm sra}$, that is, $g_{\rm sra} \rightarrow g_{\rm sra} + \Delta g_{\rm sra}$. During repetitive firing, the current builds up in a sequence of steps causing the firing rate to adapt. Figures 5.6B and 5.6C compare the adapting firing pattern of a cortical neuron with the output of the model.

As discussed in chapter 1, the probability of firing for a neuron is significantly reduced for a short period of time after the appearance of an action potential. Such a refractory effect is not included in the basic integrate-and-fire model. The simplest way of including an absolute refractory period in the model is to add a condition to the basic threshold crossing rule forbidding firing for a period of time immediately after a spike. Refratoriness can be incorporated in a more realistic way by adding a conductance similar to the spike-rate adaptation conductance discussed above, but with a faster recovery time and a larger conductance increment following an action potential. With a large increment, the current can essentially clamp the neuron to $E_{\rm K}$ following a spike, temporarily preventing further firing and producing an absolute refractory period. As this conductance relaxes

back to zero, firing will be possible but initially less likely, producing a relative refractory period. When recovery is completed, normal firing can resume. Another scheme that is sometimes used to model refractory effects is to raise the threshold for action potential generation following a spike and then to allow it to relax back to its normal value. Spike-rate adaptation can also be described by using an integrated version of the integrate-and-fire model known as the spike-response model in which membrane potential wave forms are determined by summing pre-computed postsynaptic potentials and after-spike hyperpolarizations. Finally, spike-rate adaptation and other effects can be incorporated into the integrate-and-fire framework by allowing the parameters $\overline{g}_{\rm L}$ and $E_{\rm L}$ in equation 5.7 to vary with time.

5.5 Voltage-Dependent Conductances

Most of the interesting electrical properties of neurons, including their ability to fire and propagate action potentials, arise from nonlinearities associated with active membrane conductances. Recordings of the current flowing through single channels indicate that channels fluctuate rapidly between open and closed states in a stochastic manner (figure 5.7). Models of membrane and synaptic conductances must describe how the probability that a channel is in an open, ion-conducting state at any given time depends on the membrane potential (for a voltage-dependent conductance), the presence or absence of a neurotransmitter (for a synaptic conductance), or a number of other factors such as the concentration of Ca^{2+} or other messenger molecules inside the cell. In this chapter, we consider two classes of active conductances, voltage-dependent membrane conductancesand transmitter-dependent synaptic conductances.An additional type, the Ca^{2+}-dependent conductance,is considered in chapter 6.

stochastic channel

voltage-dependent, synaptic, and Ca^{2+}-dependent conductances

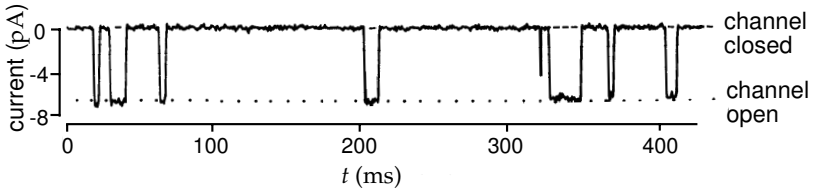

Figure 5.7: Recording of the current passing through a single ion channel. This is a synaptic receptor channel sensitive to the neurotransmitter acetylcholine. A small amount of acetylcholine was applied to the preparation to produce occasional channel openings. In the open state, the channel passes 6.6 pA at a holding potential of -140 mV. This is equivalent to more than 10^7 charges per second passing through the channel and corresponds to an open channel conductance of 47 pS. (From Hille, 1992.)

In a later section of this chapter, we discuss stochastic models of individual channels based on state diagrams and transition rates. However, most neuron models use deterministic descriptions of the conductances arising from many channels of a given type. This is justified because of the large number of channels of each type in the cell membrane of a typical neuron. If large numbers of channels are present, and if they act independently of each other (which they do, to a good approximation), then, from the law of large numbers, the fraction of channels open at any given time is approximately equal to the probability that any one channel is in an open state. This allows us to move between single-channel probabilistic formulations and macroscopic deterministic descriptions of membrane conductances.

We have denoted the conductance per unit area of membrane due to a set of ion channels of type i by g_i. The value of g_i at any given time is determined by multiplying the conductance of an open channel by the density of channels in the membrane and by the fraction of channels that are open at that time. The product of the first two factors is a constant called the maximal conductance and denoted by $\overline{g}_i$. It is the conductance per unit area of membrane if all the channels of type i are open. Maximal conductance parameters tend to range from μS/mm^2 to mS/mm^2. The fraction of channels in the open state is equivalent to the probability of finding any given channel in the open state, and it is denoted by P_i. Thus, $g_i = \overline{g}_i P_i$. The dependence of a conductance on voltage, transmitter concentration, or other factors arises through effects on the open probability.

open probability P_i

The open probability of a voltage-dependent conductance depends, as its name suggests, on the membrane potential of the neuron. In this chapter, we discuss models of two such conductances, the so-called delayed-rectifier K^+ and fast Na^+ conductances. The formalism we present, which is almost universally used to describe voltage-dependent conductances, was developed by Hodgkin and Huxley (1952) as part of their pioneering work showing how these conductances generate action potentials in the squid giant axon. Other conductances are modeled in chapter 6.

Persistent Conductances

Figure 5.8 shows cartoons of the mechanisms by which voltage-dependent channels open and close as a function of membrane potential. Channels are depicted for two different types of conductances termed persistent (figure 5.8A) and transient (figure 5.8B). We begin by discussing persistent conductances. Figure 5.8A shows a swinging gate attached to a voltage sensor that can open or close the pore of the channel. In reality, channel gating mechanisms involve complex changes in the conformational structure of the channel, but the simple swinging gate picture is sufficient if we are only interested in the current carrying capacity of the channel. A channel that acts as if it had a single type of gate (although, as we will see, this is actually modeled as a number of identical sub-gates), like the channel in figure 5.8A, produces what is called a persistent or noninactivating

activation gate

conductance. Opening of the gate is called activation of the conductance and gate closing is called deactivation. For this type of channel, the probability that the gate is open, P_K, increases when the neuron is depolarized and decreases when it is hyperpolarized. The delayed-rectifier K^+ conductance that is responsible for repolarizing a neuron after an action potential is such a persistent conductance.

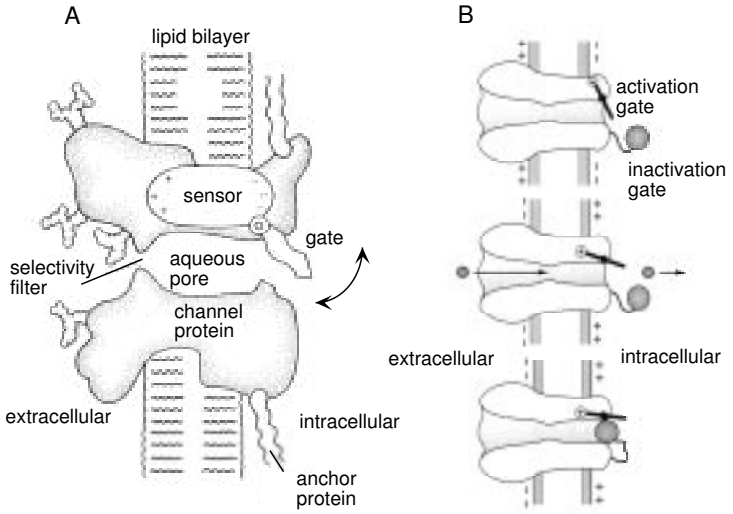

Figure 5.8: Gating of membrane channels. In both figures, the interior of the neuron is to the right of the membrane, and the extracellular medium is to the left. A) A cartoon of gating of a persistent conductance. A gate is opened and closed by a sensor that responds to the membrane potential. The channel also has a region that selectively allows ions of a particular type to pass through the channel, for example, K^+ ions for a potassium channel. B) A cartoon of the gating of a transient conductance. The activation gate is coupled to a voltage sensor (denoted by a circled +) and acts like the gate in A. A second gate, denoted by the ball, can block that channel once it is open. The top figure shows the channel in a deactivated (and deinactivated) state. The middle panel shows an activated channel, and the bottom panel shows an inactivated channel. Only the middle panel corresponds to an open, ion-conducting state. (A from Hille, 1992; B from Kandel et al., 1991.)

The opening of the gate that describes a persistent conductance may involve a number of conformational changes. For example, the delayed-rectifier K^+ conductance is constructed from four identical subunits, and it appears that all four must undergo a structural change for the channel to open. In general, if k independent, identical events are required for a channel to open, P_K can be written as

$$P_K = n^k \tag{5.15}$$

where n is the probability that any one of the k independent gating events has occurred. Here, n, which varies between 0 and 1, is called a gating

activation variable n

or an activation variable, and a description of its voltage and time dependence amounts to a description of the conductance. We can think of n as the probability of an individual subunit gate being open, and $1-n$ as the probability that it is closed.

Although using the value of $k=4$ is consistent with the four subunit structure of the delayed-rectifier conductance, in practice k is an integer chosen to fit the data, and should be interpreted as a functional definition of a subunit rather than a reflection of a realistic structural model of the channel. Indeed, the structure of the channel was not known at the time that Hodgkin and Huxley chose the form of equation 5.15 and suggested that $k=4$.

channel kinetics

We describe the transition of each subunit gate by a simple kinetic scheme in which the gating transition closed $\rightarrow$ open occurs at a voltage-dependent rate $\alpha_n(V)$, and the reverse transition open $\rightarrow$ closed occurs at a voltage-dependent rate $\beta_n(V)$. The probability that a subunit gate opens over a short interval of time is proportional to the probability of finding the gate closed, $1-n$, multiplied by the opening rate $\alpha_n(V)$. Likewise, the probability that a subunit gate closes during a short time interval is proportional to the probability of finding the gate open, n, multiplied by the closing rate $\beta_n(V)$. The rate at which the open probability for a subunit gate changes is given by the difference of these two terms

$$\frac{dn}{dt} = \alpha_n(V)(1-n) - \beta_n(V)n. \tag{5.16}$$

The first term describes the opening process and the second term the closing process (hence the minus sign) that lowers the probability of being in the configuration with an open subunit gate. Equation 5.16 can be written in another useful form by dividing through by $\alpha_n(V)+\beta_n(V)$,

gating equation

$$\tau_n(V)\frac{dn}{dt} = n_\infty(V) - n\,, \tag{5.17}$$

$\tau_n(V)$

where

$$\tau_n(V) = \frac{1}{\alpha_n(V)+\beta_n(V)} \tag{5.18}$$

$n_\infty(V)$

and

$$n_\infty(V) = \frac{\alpha_n(V)}{\alpha_n(V)+\beta_n(V)}. \tag{5.19}$$

Equation 5.17 indicates that for a fixed voltage V, n approaches the limiting value $n_\infty(V)$ exponentially with time constant $\tau_n(V)$.

The key elements in the equation that determines n are the opening and closing rate functions $\alpha_n(V)$ and $\beta_n(V)$. These are obtained by fitting experimental data. It is useful to discuss the form that we expect these rate functions to take on the basis of thermodynamic arguments. The state

transitions described by α_n, for example, are likely to be rate-limited by barriers requiring thermal energy. These transitions involve the movement of charged components of the gate across part of the membrane, so the height of these energy barriers should be affected by the membrane potential. The transition requires the movement of an effective charge, which we denote by qB_α, through the potential V. This requires an energy $qB_\alpha V$. The constant B_α reflects both the amount of charge being moved and the distance over which it travels. The probability that thermal fluctuations will provide enough energy to surmount this energy barrier is proportional to the Boltzmann factor, $\exp(-qB_\alpha V/k_B T)$. Based on this argument, we expect α_n to be of the form

$$\alpha_n(V) = A_\alpha \exp(-qB_\alpha/k_B T) = A_\alpha \exp(-B_\alpha V/V_T) \tag{5.20}$$

for some constant A_α. The closing rate β_n should be expressed similarly, except with different constants A_β and B_β. From equation 5.19, we then find that $n_\infty(V)$ is expected to be a sigmoidal function

$$n_\infty(V) = \frac{1}{1 + (A_\beta/A_\alpha)\exp((B_\alpha - B_\beta)V/V_T)}\,. \tag{5.21}$$

For a voltage-activated conductance, depolarization causes n to grow toward one, and hyperpolarization causes them to shrink toward zero. Thus, we expect that the opening rate, α_n should be an increasing function of V (and thus $B_\alpha < 0$) and β_n should be a decreasing function of V (and thus $B_\beta > 0$). Examples of the functions we have discussed are plotted in figure 5.9.

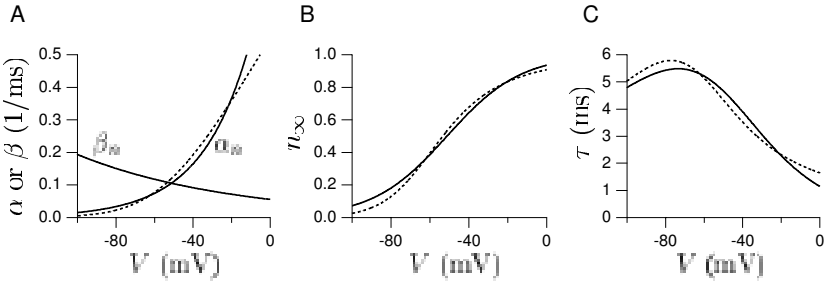

Figure 5.9: Generic voltage-dependent gating functions compared with Hodgkin-Huxley results for the delayed-rectifier K^+ conductance. A) The exponential α_n and β_n functions expected from thermodynamic arguments are indicated by the solid curves. Parameter values used were $A_\alpha = 1.22$ ms^{-1}, $A_\beta = 0.056$ ms^{-1}, $B_\alpha/V_T = -0.04$/mV, and $B_\beta/V_T = 0.0125$/mV. The fit of Hodgkin and Huxley for β_n is identical to the solid curve shown. The Hodgkin-Huxley fit for α_n is the dashed curve. B) The corresponding function $n_\infty(V)$ of equation 5.21 (solid curve). The dashed curve is obtained using the α_n and β_n functions of the Hodgkin-Huxley fit (equation 5.22). C) The corresponding function $\tau_n(V)$ obtained from equation 5.18 (solid curve). Again the dashed curve is the result of using the Hodgkin-Huxley rate functions.

voltage clamping

While thermodynamic arguments support the forms we have presented, they rely on simplistic assumptions. Not surprisingly, the resulting functional forms do not always fit the data and various alternatives are often employed. The data upon which these fits are based are typically obtained using a technique called voltage clamping. In this techniques, an amplifier is configured to inject the appropriate amount of electrode current to hold the membrane potential at a constant value. By current conservation, this current is equal to the membrane current of the cell. Hodgkin and Huxley fit the rate functions for the delayed-rectifier K^+ conductance they studied using the equations

$$\alpha_n = \frac{.01(V+55)}{1-\exp(-.1(V+55))} \quad \text{and} \quad \beta_n = 0.125\exp(-0.0125(V+65)) \tag{5.22}$$

where V is expressed in mV, and α_n and β_n are both expressed in units of 1/ms. The fit for β_n is exactly the exponential form we have discussed with $A_\beta = 0.125\exp(-0.0125 \cdot 65)$ ms^{-1} and $B_\beta / V_T = 0.0125$ mV^{-1}, but the fit for α_n uses a different functional form. The dashed curves in figure 5.9 plot the formulas of equation 5.22.

Transient Conductances

Some channels only open transiently when the membrane potential is depolarized because they are gated by two processes with opposite voltage-dependences. Figure 5.8B is a schematic of a channel that is controlled by two gates and generates a transient conductance. The swinging gate in figure 5.8B behaves exactly like the gate in figure 5.8A. The probability that it is open is written as m^k where m is an activation variable similar to n, and k is an integer. Hodgkin and Huxley used $k = 3$ for their model of the fast Na^+ conductance. The ball in figure 5.8B acts as the second gate. The probability that the ball does not block the channel pore is written as h and called the inactivation variable. The activation and inactivation variables m and h are distinguished by having opposite voltage dependences. Depolarization causes m to increase and h to decrease, and hyperpolarization decreases m while increasing h.

activation variable m

inactivation variable h

For the channel in figure 5.8B to conduct, both gates must be open, and, assuming the two gates act independently, this has probability

$$P_{\rm Na} = m^k h\,, \tag{5.23}$$

This is the general form used to describe the open probability for a transient conductance. We could raise the h factor in this expression to an arbitrary power as we did for m, but we leave out this complication to streamline the discussion. The activation m and inactivation h, like all gating variables, vary between zero and one. They are described by equations identical to 5.16, except that the rate functions α_n and β_n are replaced by

either α_m and β_m or α_h and β_h. These rate functions were fit by Hodgkin and Huxley using the equations (in units of 1/ms with V in mV)

$$\alpha_m = \frac{.1(V+40)}{1-\exp[-.1(V+40)]} \qquad \beta_m = 4\exp[-.0556(V+65)]$$
$$\alpha_h = .07\exp[-.05(V+65)] \quad \beta_h = 1/(1+\exp[-.1(V+35)])\,. \quad (5.24)$$

Functions $m_\infty(V)$ and $h_\infty(V)$ describing the steady-state activation and inactivation levels, and voltage-dependent time constants for m and h can be defined as in equations 5.19 and 5.18. These are plotted in figure 5.10. For comparison, $n_\infty(V)$ and $\tau_n(V)$ for the K^+ conductance are also plotted. Note that $h_\infty(V)$, because it corresponds to an inactivation variable, is flipped relative to $m_\infty(V)$ and $n_\infty(V)$, so that it approaches one at hyperpolarized voltages and zero at depolarized voltages.

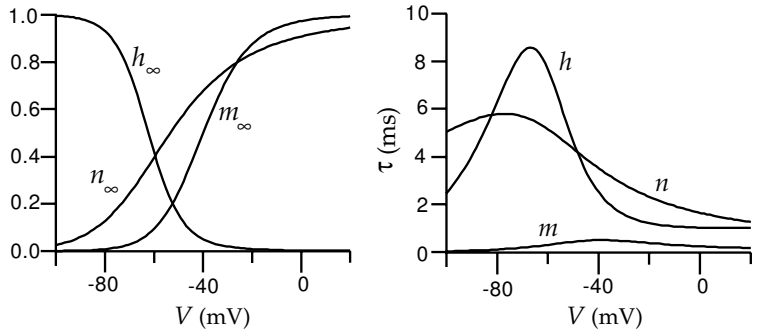

Figure 5.10: The voltage-dependent functions of the Hodgkin-Huxley model. The left panel shows $m_\infty(V)$, $h_\infty(V)$, and $n_\infty(V)$, the steady-state levels of activation and inactivation of the Na^+ conductance and activation of the K^+ conductance. The right panel shows the voltage-dependent time constants that control the rates at which these steady-state levels are approached for the three gating variables.

The presence of two factors in equation (5.23) gives a transient conductance some interesting properties. To turn on a transient conductance maximally, it may first be necessary to hyperpolarize the neuron below its resting potential and then to depolarize it. Hyperpolarization raises the value of the inactivation h, a process called deinactivation. The second step, depolarization, increases the value of m, a process known as activation. Only when m and h are both nonzero is the conductance turned on. Note that the conductance can be reduced in magnitude either by decreasing m or h. Decreasing h is called inactivation to distinguish it from decreasing m, which is called deactivation.

deinactivation
activation
inactivation
deactivation

Hyperpolarization-Activated Conductances

Persistent currents act as if they are controlled by an activation gate, while transient currents acts as if they have both an activation and an inactiva-

tion gate. Another class of conductances, the hyperpolarization-activated conductances, behave as if they are controlled solely by an inactivation gate. They are thus persistent conductances, but they open when the neuron is hyperpolarized rather than depolarized. The opening probability for such channels is written solely of an inactivation variable similar to h. Strictly speaking these conductances deinactivate when they turn on and inactivate when they turn off. However, most people cannot bring themselves to say deinactivate all the time, so they say instead that these conductances are activated by hyperpolarization.

5.6 The Hodgkin-Huxley Model

The Hodgkin-Huxley model for the generation of the action potential, in its single-compartment form, is constructed by writing the membrane current in equation 5.6 as the sum of a leakage current, a delayed-rectified K^+ current and a transient Na^+ current,

$$i_m = \overline{g}_L(V - E_L) + \overline{g}_K n^4(V - E_K) + \overline{g}_{Na} m^3 h(V - E_{Na}) . \qquad (5.25)$$

The maximal conductances and reversal potentials used in the model are $\overline{g}_L = 0.003$ mS/mm^2, $\overline{g}_K = 0.036$ mS/mm^2, $\overline{g}_{Na} = 1.2$ mS/mm^2, E_L = -54.402 mV, E_K = -77 mV and E_{Na} = 50 mV. The full model consists of equation 5.6 with equation 5.25 for the membrane current, and equations of the form 5.17 for the gating variables n, m, and h. These equations can be integrated numerically using the methods described in appendices A and B.

The temporal evolution of the dynamic variables of the Hodgkin-Huxley model during a single action potential is shown in figure 5.11. The initial rise of the membrane potential, prior to the action potential, seen in the upper panel of figure 5.11, is due to the injection of a positive electrode current into the model starting at $t = 5$ ms. When this current drives the membrane potential up to about about -50 mV, the m variable that describes activation of the Na^+ conductance suddenly jumps from nearly zero to a value near one. Initially, the h variable, expressing the degree of inactivation of the Na^+ conductance, is around 0.6. Thus, for a brief period both m and h are significantly different from zero. This causes a large influx of Na^+ ions producing the sharp downward spike of inward current shown in the second trace from the top. The inward current pulse causes the membrane potential to rise rapidly to around 50 mV (near the Na^+ equilibrium potential). The rapid increase in both V and m is due to a positive feedback effect. Depolarization of the membrane potential causes m to increase, and the resulting activation of the Na^+ conductance causes V to increase. The rise in the membrane potential causes the Na^+ conductance to inactivate by driving h toward zero. This shuts off the Na^+ current. In addition, the rise in V activates the K^+ conductance by driving n toward one. This increases the K^+ current which drives the membrane

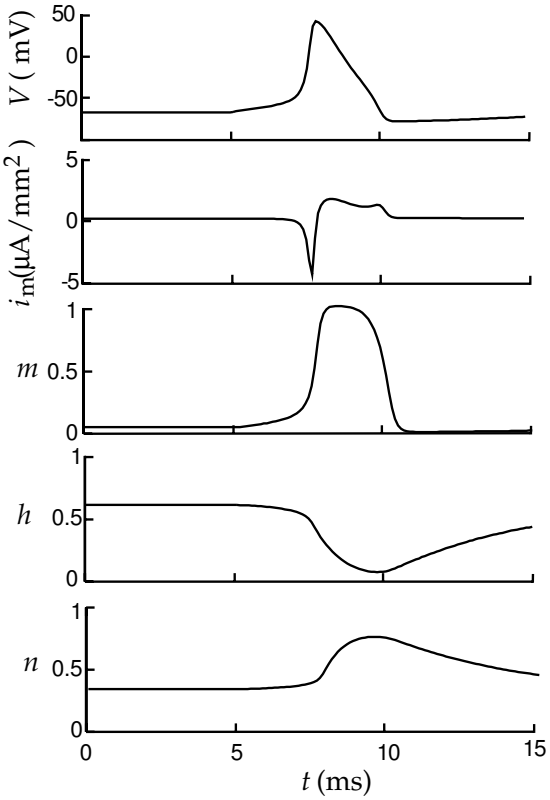

Figure 5.11: The dynamics of V, m, h, and n in the Hodgkin-Huxley model during the firing of an action potential. The upper trace is the membrane potential, the second trace is the membrane current produced by the sum of the Hodgkin-Huxley K^+ and Na^+ conductances, and subsequent traces show the temporal evolution of m, h, and n. Current injection was initiated at $t = 5$ ms.

potential back down to negative values. The final recovery involves the re-adjustment of m, h, and n to their initial values.

The Hodgkin-Huxley model can also be used to study propagation of an action potential down an axon, but for this purpose a multi-compartment model must be constructed. Methods for constructing such a model, and results from it, are described in chapter 6.

5.7 Modeling Channels

In previous sections, we described the Hodgkin-Huxley formalism for describing voltage-dependent conductances arising from a large number of channels. With the advent of single channel studies, microscopic de-

scriptions of the transitions between the conformational states of channel molecules have been developed. Because these models describe complex molecules, they typically involve many states and transitions. Here, we discuss simple versions of these models that capture the spirit of single-channel modeling without getting mired in the details.

Models of single channels are based on state diagrams that indicate the possible conformational states that the channel can assume. Typically, one of the states in the diagram is designated as open and ion-conducting, while the other states are non-conducting. The current conducted by the channel is written as $\overline{g}P(V-E)$, where E is the reversal potential, $\overline{g}$ is the single-channel open conductance and P is one whenever the open state is occupied and zero otherwise. Channel models can be instantiated directly from state diagrams simply by keeping track of the state of the channel and allowing stochastic changes of state to occur at appropriate transition rates. If the model is updated in short time steps of duration Δt, the probability that the channel makes a given transition during an update interval is the transition rate times Δt.

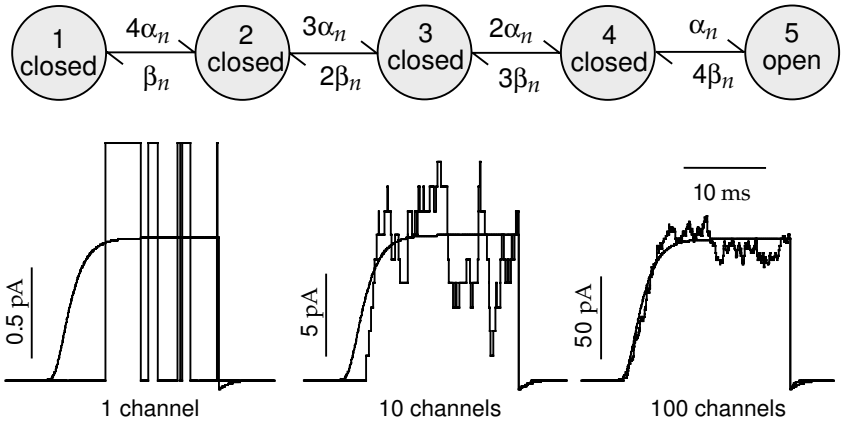

Figure 5.12: A model of the delayed-rectifier K^+ channel. The upper diagram shows the states and transition rates of the model. In the simulations shown in the lower panels, the membrane potential was initially held at -100 mV, then held at 10 mV for 20 ms, and finally returned to a holding potential of -100 mV. The smooth curves in these panels show the membrane current predicted by the Hodgkin-Huxley model in this situation. The left panel shows a simulation of a single channel that opened several times during the depolarization. The middle panel shows the total current from 10 simulated channels and the right panel corresponds to 100 channels. As the number of channels increases, the Hodgkin-Huxley model provides a more accurate description of the current.

Figure 5.12 shows the state diagram and simulation results for a model of a single delayed-rectifier K^+ channel that is closely related to the Hodgkin-Huxley description of the macroscopic delayed-rectifier conductance. The factors α_n and β_n in the transition rates shown in the state diagram of fig-

ure 5.12 are the voltage-dependent rate functions of the Hodgkin-Huxley model. The model uses the same four subunit structure assumed in the Hodgkin-Huxley model. We can think of state 1 in this diagram as a state in which all the subunit gates are closed. States 2, 3, 4, and 5 have 1, 2, 3, and 4 open subunit gates respectively. State 5 is the sole open state. The factors of 1, 2, 3, and 4 in the transition rates in figure 5.12 correspond to the number of subunit gates that can make a given transition. For example, the transition rate from state 1 to state 2 is four times faster than the rate from state 4 to state 5. This is because any one of the 4 subunit gates can open to get from state 1 to state 2, but the transition from state 4 to state 5 requires the single remaining closed subunit gate to open.

The lower panels in figure 5.12 show simulations of this model involving 1, 10, and 100 channels. The sum of currents from all of these channels is compared with the current predicted by the Hodgkin-Huxley model (scaled by the appropriate maximal conductance). For each channel, the pattern of opening and closing is random, but when enough channels are summed, the total current matches that of the Hodgkin-Huxley model quite well.

To see how the channel model in figure 5.12 reproduces the results of the Hodgkin-Huxley model when the currents from many channels are summed, we must consider a probabilistic description of the channel model. We denote the probability that a channel is in state a of figure 5.12 by p_a, with $a = 1, 2, \ldots, 5$. Dynamic equations for these probabilities are easily derived by setting the rate of change for a given p_a equal to the probability per unit time of entry into state a from other states minus the rate for leaving a state. The entry probability per unit time is the product of the appropriate transition rate times the probability that the state making the transition is occupied. The probability per unit time for leaving is p_a times the sum of all the rates for possible transitions out of the state. Following this reasoning, the equations for the state probabilities are

$$\begin{aligned}
\frac{dp_1}{dt} &= \beta_n p_2 - 4\alpha_n p_1 \qquad (5.26)\\
\frac{dp_2}{dt} &= 4\alpha_n p_1 + 2\beta_n p_3 - (\beta_n + 3\alpha_n) p_2\\
\frac{dp_3}{dt} &= 3\alpha_n p_2 + 3\beta_n p_4 - (2\beta_n + 2\alpha_n) p_3\\
\frac{dp_4}{dt} &= 2\alpha_n p_3 + 4\beta_n p_5 - (3\beta_n + \alpha_n) p_4\\
\frac{dp_5}{dt} &= \alpha_n p_4 - 4\beta_n p_5 \,.
\end{aligned}$$

A solution for these equations can be constructed if we recall that, in the Hodgkin-Huxley model, n is the probability of a subunit gate being in the open state and $1 - n$ the probability of it being closed. If we use that same notation here, state 1 has 4 closed subunit gates, and thus $p_1 = (1 - n)^4$. State 5, the open state, has 4 open subunit gates so $p_5 = n^4 = P$. State

2 has one open subunit gate, which can be any one of the four subunit gates, and three closed states making $p_2 = 4n(1-n)^3$. Similar arguments yield $p_3 = 6n^2(1-n)^2$ and $p_4 = 4n^3(1-n)$. These expressions generate a solution to the above equations provided that n satisfies equation 5.16, as the reader can verify.

In the Hodgkin-Huxley model of the Na^+ conductance, the activation and inactivation processes are assumed to act independently. The schematic in figure 5.8B, which cartoons the mechanism believed to be responsible for inactivation, suggests that this assumption is incorrect. The ball that inactivates the channel is located inside the cell membrane where it cannot be affected directly by the potential across the membrane. Furthermore, in this scheme, the ball cannot occupy the channel pore until the activation gate has opened, making the two processes inter-dependent.

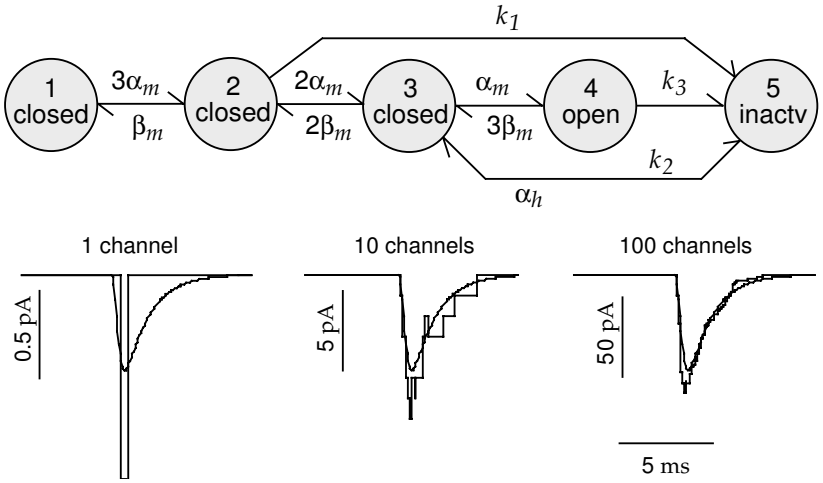

Figure 5.13: A model of the fast Na^+ channel. The upper diagram shows the states and transitions rates of the model. The values $k_1 = 0.24$/ms, $k_2 = 0.4$/ms, and $k_3 = 1.5$/ms were used in the simulations shown in the lower panels. For these simulations, the membrane potential was initially held at -100 mV, then held at 10 mV for 20 ms, and finally returned to a holding potential of -100 mV. The smooth curves in these panels show the current predicted by the Hodgkin-Huxley model in this situation. The left panel shows a simulation of a single channel that opened once during the depolarization. The middle panel shows the total current from 10 simulated channels and the right panel corresponds to 100 channels. As the number of channels increases, the Hodgkin-Huxley model provides a fairly accurate description of the current, but it is not identical to the channel model in this case.

state-dependent inactivation

The state diagram in figure 5.13 reflects this by having a state-dependent, voltage-independent inactivation mechanism. This diagram is a simplified version of a Na^+ channel model due to Patlak (1991). The sequence of transitions that lead to channel opening through states 1 ,2, 3, and 4 is identical to that of the Hodgkin-Huxley model with transition rates deter-

mined by the Hodgkin-Huxley functions $\alpha_m(V)$ and $\beta_m(V)$ and appropriate combinatoric factors. State 4 is the open state. The transition to the inactivated state 5, however, is quite different from the inactivation process in the Hodgkin-Huxley model. Inactivation transitions to state 5 can only occur from states 2, 3, and 4, and the corresponding transition rates k_1, k_2, and k_3 are constants, independent of voltage. The deinactivation process occurs at the Hodgkin-Huxley rate $\alpha_h(V)$ from state 5 to state 3.

Figure 5.13 shows simulations of this Na^+ channel model. In contrast to the K^+ channel model shown in figure 5.12, this model does not reproduce exactly the results of the Hodgkin-Huxley model when large numbers of channels are summed. Nevertheless, the two models agree quite well, as seen in the lower right panel of figure 5.13. The agreement, despite the different mechanisms of inactivation, is due to the speed of the activation process for the Na^+ conductance. The inactivation rate function $\beta_h(V)$ in the Hodgkin-Huxley model has a sigmoidal form similar to the asymptotic activation function $m_\infty(V)$ (see equation 5.24). This is indicative of the actual dependence of inactivation on m and not V. However, the activation variable m of the Hodgkin-Huxley model reaches its voltage-dependent asymptotic value $m_\infty(V)$ so rapidly that it is difficult to distinguish inactivation processes that depend on m from those that depend on V. Differences between the two models are only apparent during a sub-millisecond time period while the conductance is activating. Experiments that can resolve this time scale support the channel model over the original Hodgkin-Huxley description.

5.8 Synaptic Conductances

Synaptic transmission at a spike-mediated chemical synapse begins when an action potential invades the presynaptic terminal and activates voltage-dependent Ca^{2+} channels leading to a rise in the concentration of Ca^{2+} within the terminal. This causes vesicles containing transmitter molecules to fuse with the cell membrane and release their contents into the synaptic cleft between the pre- and postsynaptic sides of the synapse. The transmitter molecules then diffuse across the cleft and bind to receptors on the postsynaptic neuron. Binding of transmitter molecules leads to the opening of ion channels that modify the conductance of the postsynaptic neuron, completing the transmission of the signal from one neuron to the other. Postsynaptic ion channels can be activated directly by binding to the transmitter, or indirectly when the transmitter binds to a distinct receptor that affects ion channels through an intracellular second-messenger signaling pathway.

As with a voltage-dependent conductance, a synaptic conductance can be written as the product of a maximal conductance and an open channel probability, $g_s = \overline{g}_s P$. The open probability for a synaptic conductance can be expressed as a product of two terms that reflect processes occurring on